



HAL
open science

Dense stellar matter with trapped neutrinos under strong magnetic fields

Aziz Rabhi, Constança Providência

► **To cite this version:**

Aziz Rabhi, Constança Providência. Dense stellar matter with trapped neutrinos under strong magnetic fields. *Journal of Physics G: Nuclear and Particle Physics*, 2010, 37 (7), pp.75102. 10.1088/0954-3899/37/7/075102 . hal-00600818

HAL Id: hal-00600818

<https://hal.science/hal-00600818>

Submitted on 16 Jun 2011

HAL is a multi-disciplinary open access archive for the deposit and dissemination of scientific research documents, whether they are published or not. The documents may come from teaching and research institutions in France or abroad, or from public or private research centers.

L'archive ouverte pluridisciplinaire **HAL**, est destinée au dépôt et à la diffusion de documents scientifiques de niveau recherche, publiés ou non, émanant des établissements d'enseignement et de recherche français ou étrangers, des laboratoires publics ou privés.

Dense stellar matter with trapped neutrinos under strong magnetic fields

Aziz Rabhi^{1,2,*} and Constança Providência^{1,†}¹*Centro de Física Computacional, Department of Physics,
University of Coimbra, 3004-516 Coimbra, Portugal*²*Laboratoire de Physique de la Matière Condensée,
Faculté des Sciences de Tunis, Campus Universitaire, Le Belvédère-1060, Tunisia*

(Dated: December 17, 2009)

We investigate the effects of strong magnetic fields on the equation of state of dense stellar neutrino-free and neutrino-trapped matter. Relativistic nuclear models both with constant couplings (NLW) and with density dependent parameters (DDRH) and including hyperons are considered. It is shown that at low densities neutrinos are suppressed in the presence of the magnetic field. The magnetic field reduces the strangeness fraction of neutrino-free matter and increases the strangeness fraction of neutrino-trapped matter. We have studied some properties of stars with trapped neutrinos and strong magnetic fields. A density dependent magnetic field with the magnitude 10^{15} G at the surface was considered. The magnetic field reduces the strangeness content of the star, and, as a consequence, the possibility of formation of a black-hole after the outflow of neutrinos, since it is the appearance of exotic matter in neutrino free matter that may induce a black-hole formation, if the EOS becomes too soft.

PACS numbers: 26.60.+c, 12.39.Ba, 21.65.+f, 97.60.Jd

I. INTRODUCTION

Neutron stars with very strong magnetic fields of the order of $10^{14} - 10^{15}$ G are known as magnetars [1–3]. They are believed to be the sources of the intense γ and X rays (for a review refer to [4]). Although until presently only 16 magnetars have been identified as short γ -ray repeaters or anomalous X-ray pulsars [5], according to Ref. [6], a fraction as high as 10% of the neutron star population could be magnetars. Magnetars are warm, young stars, ~ 1 kyear old.

The study of dense stellar matter under strong magnetic fields is, therefore of great interest. Our knowledge of neutron star composition and structure is still uncertain [7]. For densities below twice normal nuclear matter density ($\rho_0 \sim 0.153 \text{ fm}^{-3}$), the matter consists only of nucleons and leptons. For baryon densities above $2\rho_0$, the equation of state (EOS) and the composition of matter are much less certain and the strangeness degree of freedom should be taken into account either through the onset of hyperons, kaon condensation or a deconfinement phase transition into strange quark matter. The presence of hyperons in neutron stars, which has been studied by many authors [8–18], tends to soften the EOS at high density and lower the maximum mass of neutron stars [9, 14–19]. Cold dense stellar matter is neutrino free but the protoneutron star formed after a supernova explosion, with an entropy per baryon of the order of 1 to 2, contains trapped neutrinos. After 10 to 20 s, the star stabilizes at practically zero temperature and no trapped neutrinos are left [20].

In this article, we focus on the properties of hyperonic matter, which is composed of a chemically equilibrated and charge-neutral mixture of nucleons, hyperons, and leptons. The meson-hyperon couplings play an important role in the determination of the EOS and the composition of hyperonic matter. In the presence of strong magnetic fields, the pressure and composition of matter can be affected significantly [21]. In Ref. [21], the authors have investigated the effects of strong magnetic fields on the properties of neutron star matter including hyperons, but no neutrino trapping was considered. It was found that the EOS at high density could be significantly affected both by Landau quantization and by the magnetic moment interactions, but only for field strength $B > 5 \times 10^{18}$ G. They have studied the neutron star structure using general relativistic magneto-hydrostatic calculations and have demonstrated that the maximum average fields within a stable neutron are limited to values $B \sim 1 - 3 \times 10^{18} \text{ G}$. These values agree with the ones obtained from the scalar virial theorem according to which the maximum interior field strength could be as large as 10^{18} G for a compact star [22].

In Ref. [21], it was also shown that the threshold densities of hyperons can be significantly altered by strong magnetic

*Electronic address: rabhi@teor.fis.uc.pt

†Electronic address: cp@teor.fis.uc.pt

field. Similar conclusions were obtained in [23] where the strangeness was included through an antikaon condensation or in [24] where not only hyperons but also the strange mesons σ^* and ϕ were included in the EOS.

We wish to investigate the influence of strong magnetic fields on hyperonic matter when neutrinos are trapped. Although, we should consider warm matter, it was shown [20, 25] that the effect of the inclusion of trapped neutrinos is more important than the temperature effect. While the presence of neutrinos has a strong effect on the structure of the star, the temperature has almost no effect on the maximum star mass configuration and a calculation done at zero temperature predicts for hadronic stars just slightly larger gravitational masses, less than 1% larger, and slightly smaller radius, $\sim 1\%$ smaller. We expect, therefore, that the main conclusions taken for $T = 0$ will still be valid at finite temperature. Similar studies at zero temperature have been done by other authors when investigating the effect of neutrinos on the compact star structure [26]. It should, however, be pointed out that the temperature will bring the onset of strangeness to lower densities although the overall fraction of strangeness will not change much. In a future work a finite temperature calculation will complete the present work.

For matter without a strong magnetic field, it has been shown in Ref. [20, 25] that if stellar matter is described using an EOS with hyperons the inclusion of trapped neutrinos gives an harder EOS than the neutrino-free EOS, and, therefore, the maximum baryonic allowed mass of a stable star is higher when neutrinos are trapped. As a consequence, after the neutrino outflow has occurred the most massive stars may decay into a blackhole. This is not anymore true for a stellar matter EOS with no strangeness. In this case, neutrinos make the EOS softer [20]. However, we will not discuss this case in the present work.

The effect of the magnetic field on the structure and composition of a neutron star allowing quark-hadron phase transition with trapped neutrinos has been studied in Ref. [27]. They have concluded that the strong magnetic field makes the overall equation of state softer giving rise to much smaller maximum mass configurations which do not favor the formation of low mass black-holes. Their conclusion about the reduction of the maximum mass configuration is in contrast with the result from other works [21, 28] where an increase is predicted due to the positive contribution of the magnetic field pressure to the total EOS. In Ref. [27] the magnetic field pressure enters the total EOS as a negative contribution, making the overall EOS softer.

This work is organized as follows: we make a brief review of the formalism used for the hadron matter with and without trapped neutrinos. Next we present and discuss the results obtained for the equation of state of stellar matter and the consequence on the properties of compact stars, for several values of the magnetic field. At the end we will draw some conclusions.

II. THE FORMALISM

For the description of the neutron star matter, we employ the standard mean-field theory (MFT) approach. A complete set of the equations and the description of the method can be found in Ref. [29, 30]. The Lagrangian density of the relativistic TW model [31, 32] is given by

$$\begin{aligned}
\mathcal{L} = & \sum_b \bar{\Psi}_b \left[i\gamma_\mu \partial^\mu - q_b \gamma_\mu A^\mu - m_b + \Gamma_{\sigma b} \sigma \right. \\
& \left. - \Gamma_{\omega b} \gamma_\mu \omega^\mu - \Gamma_{\rho b} \tau_{3b} \gamma_\mu \rho^\mu - \frac{1}{2} \mu_N \kappa_b \sigma_{\mu\nu} F^{\mu\nu} \right] \Psi_b \\
& + \sum_l \bar{\psi}_l (i\gamma_\mu \partial^\mu - q_l \gamma_\mu A^\mu - m_l) \psi_l \\
& + \frac{1}{2} \partial_\mu \sigma \partial^\mu \sigma - \frac{1}{2} m_\sigma^2 \sigma^2 + \frac{1}{2} m_\omega^2 \omega_\mu \omega^\mu - \frac{1}{4} \Omega^{\mu\nu} \Omega_{\mu\nu} \\
& - \frac{1}{4} F^{\mu\nu} F_{\mu\nu} + \frac{1}{2} m_\rho^2 \rho_\mu \rho^\mu - \frac{1}{4} \mathbf{P}^{\mu\nu} \mathbf{P}_{\mu\nu}
\end{aligned} \tag{1}$$

where Ψ_b and ψ_l are the baryon and lepton Dirac fields, respectively. The index b runs over the eight lightest baryons n , p , Λ , Σ^- , Σ^0 , Σ^+ , Ξ^- and Ξ^0 (neglecting the Ω^- and the Δ quartet, which appear only at quite high densities, does not qualitatively affect our conclusions), and the sum on l is over electrons and muons (e^- and μ^-). σ , ω , and ρ represent the scalar, vector, and isovector-vector meson fields, which are exchanged for the description of nuclear interactions and $A^\mu = (0, 0, Bx, 0)$ refers to a external magnetic field along the z-axis. The baryon mass and isospin projection are denoted by m_b and τ_{3b} , respectively. The mesonic and electromagnetic field strength tensors are given by their usual expressions: $\Omega_{\mu\nu} = \partial_\mu \omega_\nu - \partial_\nu \omega_\mu$, $\mathbf{P}_{\mu\nu} = \partial_\mu \rho_\nu - \partial_\nu \rho_\mu$, and $F_{\mu\nu} = \partial_\mu A_\nu - \partial_\nu A_\mu$. The baryon anomalous magnetic moments (AMM) are introduced via the coupling of the baryons to the electromagnetic field tensor with $\sigma_{\mu\nu} = \frac{i}{2} [\gamma_\mu, \gamma_\nu]$ and strength $\kappa_b = (\mu_b / \mu_N - q_b m_p / m_b)$. We neglect the AMM of the leptons in this work, because their effect is very small as shown in Ref. [33]. For the electromagnetic field, only frozen-field configurations are

TABLE I: Static properties of the baryons considered in this study. The mass, electric charge and strange charge of the baryon b are denoted by m_b , q_b and q_b^s , respectively. The baryonic magnetic moment is denoted by μ_b and the anomalous magnetic moment by $\kappa_b = (\mu_b/\mu_N - q_b m_p/m_b)$, where μ_N is the nuclear magneton.

baryon name	Mass (MeV)	Charge $q_b(e)$	Strangeness q_b^s	Magnetic moment μ_b/μ_N	Anomalous magnetic moment κ_b
p	938.27	1	0	2.97	1.79
n	939.56	0	0	-1.91	-1.91
Λ^0	1115.7	0	-1	-0.61	-0.61
Σ^+	1189.4	1	-1	2.46	1.67
Σ^0	1192.6	0	-1	1.61	1.61
Σ^-	1197.4	-1	-1	-1.16	-038
Ξ^0	1314.8	0	-2	-1.25	-1.25
Ξ^-	1321.3	-1	-2	-0.65	0.06

considered and thus there is no associated field equation. The density dependent strong interaction couplings are denoted by Γ , the electromagnetic couplings by q and the baryons, mesons and leptons masses by m . The parameters of the model are the nucleon mass $M = 939$ MeV, the masses of mesons m_σ , m_ω , m_ρ and the density dependent coupling parameters which are adjusted in order to reproduce some of the nuclear matter bulk properties and relations with the Dirac-Brueckner Hartree-Fock (DBHF) calculations [34], using the following parametrisation

$$\Gamma_i(\rho) = \Gamma_i(\rho_0) f_i(x), \quad i = \sigma, \omega \quad (2)$$

with

$$f_i(x) = a_i \frac{1 + b_i (x + d_i)^2}{1 + c_i (x + d_i)^2} \quad (3)$$

where $x = \rho/\rho_0$ and

$$\Gamma_\rho(\rho) = \Gamma_\rho(\rho_0) \exp[-a_\rho(x - 1)] \quad (4)$$

with the values of the parameters m_i , Γ_i , a_i , b_i , c_i and d_i , $i = \sigma, \omega, \rho$ given in [32]. The meson-hyperon couplings are assumed to be fixed fractions of the meson-nucleon couplings, $\Gamma_{iH} = x_{iH} \Gamma_{iN}$, where for each meson i , the values of x_{iH} are assumed equal for all hyperons H . Glendenning and Moszkowski [35] have constrained the x_{iH} values by neutron star maximum masses and the binding energy of the Λ at nuclear saturation. Two possible sets of x_{iH} are given in Table II and will be identified by the x_σ value, 0.6 and 0.8. Other hypernuclear potentials in nuclear matter, consistent with hypernuclear data [36–38], may be used to constrain further the sigma-hyperon couplings. This was done in [39] where, following Ref. [37] the values for the hypernuclear potentials, $V_\Lambda = -28$ MeV, $V_\Sigma = 30$ MeV, $V_\Xi = -18$ MeV, have been used. While the main conclusions with respect to the strangeness content of the EOS do not differ when the last parametrization is used instead of the ones proposed in [35] with $x_\sigma = 0.6$ or 0.8, the onset of each hyperon species will depend on the parametrization: with the parametrization of Glendenning and Moszkowski [35] the Σ^- and the Λ are the first hyperons to appear as the density increases while using the parametrization proposed in [39] the first hyperons are Λ and Ξ^- .

For GM1 model, we add to the Lagrangian density, Eq. (1), the scalar meson self-interaction terms

$$\mathcal{L}_{nl\sigma} = -\frac{1}{3} b m_n (g_\sigma \sigma)^3 - \frac{1}{4} c (g_\sigma \sigma)^4,$$

where $g_i = \Gamma_i$, b and c are two dimensionless parameters.

For neutrino-free stellar matter consisting of a β -equilibrium mixture of baryons and leptons, the following equilibrium conditions must be imposed:

$$\mu_b = q_b \mu_n - q_l \mu_e, \quad (5)$$

$$\mu_\mu = \mu_e, \quad (6)$$

where μ_i is the chemical potential of species i . The electric charge neutrality condition is expressed by

$$\sum_b q_b \rho_b^v + \sum_l q_l \rho_l^v = 0, \quad (7)$$

TABLE II: Saturation properties of nuclear matter and the nucleon-meson coupling constants for the GM1 and TW models. The relative hyperon-meson coupling constants used in the calculation are also given.

Model	ρ_0 (fm)	-B/A (MeV)	M^*/M	$\Gamma_{\sigma N}/m_\sigma$ (fm)	$\Gamma_{\omega N}/m_\omega$ (fm)	$\Gamma_{\rho N}/m_\rho$ (fm)	$x_{\sigma H}$	$x_{\omega H}$	$x_{\rho H}$	b	c
GM1	0.153	16.30	0.70	3.434	2.674	2.100	0.600	0.653	0.600	0.002947	-0.001070
TW	0.153	16.30	0.56	3.84901	3.34919	1.89354	0.600	0.658	0.600	0.0	0.0
							0.800	0.913	0.800		
							0.800	0.905	0.800		

where ρ_i^v is the number density of particle i . If trapped neutrinos are included, we replace $\mu_e \rightarrow \mu_e - \mu_{\nu_e}$ in the above equations,

$$\mu_b = q_b \mu_n - q_l (\mu_e - \mu_{\nu_e}), \quad (8)$$

and for leptons we have

$$\mu_\mu - \mu_{\nu_\mu} = \mu_e - \mu_{\nu_e}. \quad (9)$$

In the above equations μ_μ, μ_{ν_e} are the chemical potential, respectively, of the muon and electron neutrinos. The introduction of additional variables, the neutrino chemical potentials, requires additional constraints, which we supply by fixing the lepton fraction $Y_{Le} = Y_e + Y_{\nu_e} = 0.4$ [20, 40]. Also, because no muons are present before and during the supernova explosion, the constraint $Y_{L\mu} = Y_\mu + Y_{\nu_\mu} = 0$ must be imposed.

For neutrino-trapped matter, the neutrino density is given by

$$\rho_{\nu_e}^v = \frac{k_F^{\nu_e 3}}{6\pi^2}. \quad (10)$$

The chemical potentials of baryons and leptons are defined as

$$\mu_b = E_F^b + \Gamma_{\omega b} \omega^0 + \Gamma_{\rho b} \tau_{3b} \rho^0 + \Sigma_0^R \quad (11)$$

$$\mu_l = E_F^l, \quad (12)$$

where the Fermi energies for charged baryons, neutral baryons and leptons (electrons and muons) are given by

$$E_F^i = \sqrt{k_F^2 + \bar{m}_i^2}, \quad i = b, l \quad (13)$$

$$(14)$$

with \bar{m}_i given by

$$\bar{m}_{b,c} = \sqrt{m_b^{*2} + 2\nu|q_b|B} - s\mu_N \kappa_b B, \quad (\text{charged baryons}) \quad (15)$$

$$\bar{m}_{b,0} = m_b^* - s\mu_N \kappa_b B, \quad (\text{neutral baryons}) \quad (16)$$

$$\bar{m}_l = \sqrt{m_l^2 + 2\nu|q_l|B} \quad (\text{charged leptons}), \quad (17)$$

where $\nu = n + \frac{1}{2} - \text{sgn}(q)\frac{s}{2} = 0, 1, 2, \dots$ enumerates the Landau levels (LL) of the fermions with electric charge q , the quantum number s is +1 for spin up and -1 for spin down cases. The rearrangement term in (11) is given by

$$\begin{aligned} \Sigma_0^R &= \sum_b \left(\frac{\partial \Gamma_{\omega b}}{\partial \rho} \rho_b^v \omega_0 + \frac{\partial \Gamma_{\rho b}}{\partial \rho} \tau_{3b} \rho_b^v \rho_0 - \frac{\partial \Gamma_{\sigma b}}{\partial \rho} \rho_b^s \sigma \right) \\ &= \frac{1}{\Gamma_{\omega N}} \frac{\partial \Gamma_{\omega N}}{\partial \rho} m_\omega^2 \omega_0^2 + \frac{1}{\Gamma_{\rho N}} \frac{\partial \Gamma_{\rho N}}{\partial \rho} m_\rho^2 \rho_0^2 - \frac{1}{\Gamma_{\sigma N}} \frac{\partial \Gamma_{\sigma N}}{\partial \rho} m_\sigma^2 \sigma^2. \end{aligned} \quad (18)$$

The pressure of neutron star matter can be obtained by

$$P_m = \sum_i \mu_i \rho_i^v - \varepsilon_m = \mu_n \sum_b \rho_b^v - \varepsilon_m \quad (19)$$

where the charge neutrality and β -equilibrium conditions are used to get the last equality. The expressions for the energy density ε_m , scalar density ρ_b^s and the particle densities ρ_i^v may be found in [30].

If the stellar matter contains neutrinos trapped, their energy density and pressure contributions, respectively,

$$\begin{aligned}\varepsilon_{\nu_e} &= \frac{k_F^{\nu_e 4}}{8\pi^2}, \\ P_{\nu_e} &= \frac{k_F^{\nu_e 4}}{24\pi^2},\end{aligned}\tag{20}$$

should be added to the stellar matter energy and pressure. The total energy density and pressure of the system includes the contribution of the magnetic field,

$$\begin{aligned}\varepsilon &= \varepsilon_m + \frac{B^2}{2}, \\ P &= P_m + \frac{B^2}{2}.\end{aligned}\tag{21}$$

With the obtained EOS, the mass-radius relation and other relevant quantities of neutron star can be derived by solving the Tolman-Oppenheimer-Volkoff (TOV) equations.

III. RESULTS AND DISCUSSION

A. Uniform magnetic field

In this section we consider that the external magnetic field is constant. The magnetic field will be defined in units of the critical field $B_e^c = 4.414 \times 10^{13}$ G, so that $B = B^* B_e^c$. In order to study the effect of strong magnetic fields on the structure of hyperonic matter we use two different relativistic mean-field approaches: the GM1 parametrisation of the NLW models [35], and the TW parametrization of the density-dependent relativistic hadronic (DDRH) models [31, 32], given in Table II. We include the baryonic octet in the EOS and choose two sets of hyperon-meson coupling constants given in Table II. The static properties of the baryons considered are listed in Table I.

In Fig. 1, the EoS obtained with both relativistic mean-field models GM1 and TW are displayed for $B^* = 0, 10^5$, and 3×10^5 , for the relative hyperon coupling constant $x_\sigma = 0.6$ (thick lines) and $x_\sigma = 0.8$ (thin lines). In Fig. 1 (a) and Fig. 1 (c) the EOS does not include the contribution from the AMM and in Fig. 1 (b) and Fig. 1 (d) the AMM was included. The kink on each one of the curves identifies the onset of hyperons. Both for TW, which gives a softer EOS, and for GM1, the EOS at higher densities are harder for $x_\sigma = 0.8$ than for $x_\sigma = 0.6$ because a larger ω or ρ coupling constant makes the onset of hyperons only possible at larger densities. This is also valid in the presence of a strong magnetic field. The effects of the AMM are only noticeable for the stronger magnetic fields. It is seen that, in the absence of the AMM and in presence of a strong magnetic field, the EOS becomes softer for the smaller densities and harder at the larger densities due to the Landau quantization which affects charged particles.

The effect of magnetic field on the EOS, when trapped neutrinos are considered, is seen in Fig. 2 for GM1 and TW models, with $x_\sigma = 0.6$ and without/with AMM. For $B = 0$ the presence of neutrinos makes the EOS harder when hyperons have been included [20, 25]. A strong magnetic field without including the AMM, makes the EOS harder at high densities if neutrino trapping is enforced. Moreover, if the AMM are included the EOS become even harder. At low densities, however, the magnetic field softens the EOS even when the AMM are taken into account. We remark that for the largest field considered and taking into account AMM, it is not possible to get an EOS at low densities for the lepton fraction $Y_L = 0.4$. In Fig. 3 we plot the baryon density threshold, at which the neutrino chemical potential vanishes, as function of the magnetic field, for GM1 and TW models using $x_\sigma = 0.6$ and without/with including AMM. Below this threshold density, it is not possible to impose the lepton fraction $Y_L = 0.4$. This happens because at low densities and for a very strong magnetic field the proton fraction of β equilibrium matter is very large. If the proton fraction is larger than 0.4, we must have an equal amount of electrons for charge neutrality and it will not be possible to get a lepton fraction 0.4 since the electrons already give a larger contribution than 0.4. The threshold density for neutrino onset increases very fast with the increase of the magnetic field, *e.g.* in Fig. 3(a) for $B^* = 5 \times 10^5$ corresponds a threshold density equal to $0.5\rho_0$ for GM1 and $1.35\rho_0$ for TW. The kink at $\rho \sim 2.5\rho_0$ corresponds to the hyperon onset. However, at the surface of the magnetar the measured magnetic fields are at most $B^* \sim 10^2$ and it is probable that even if the magnetic field is stronger in the interior it will be weaker than the threshold values given in Fig. 3.

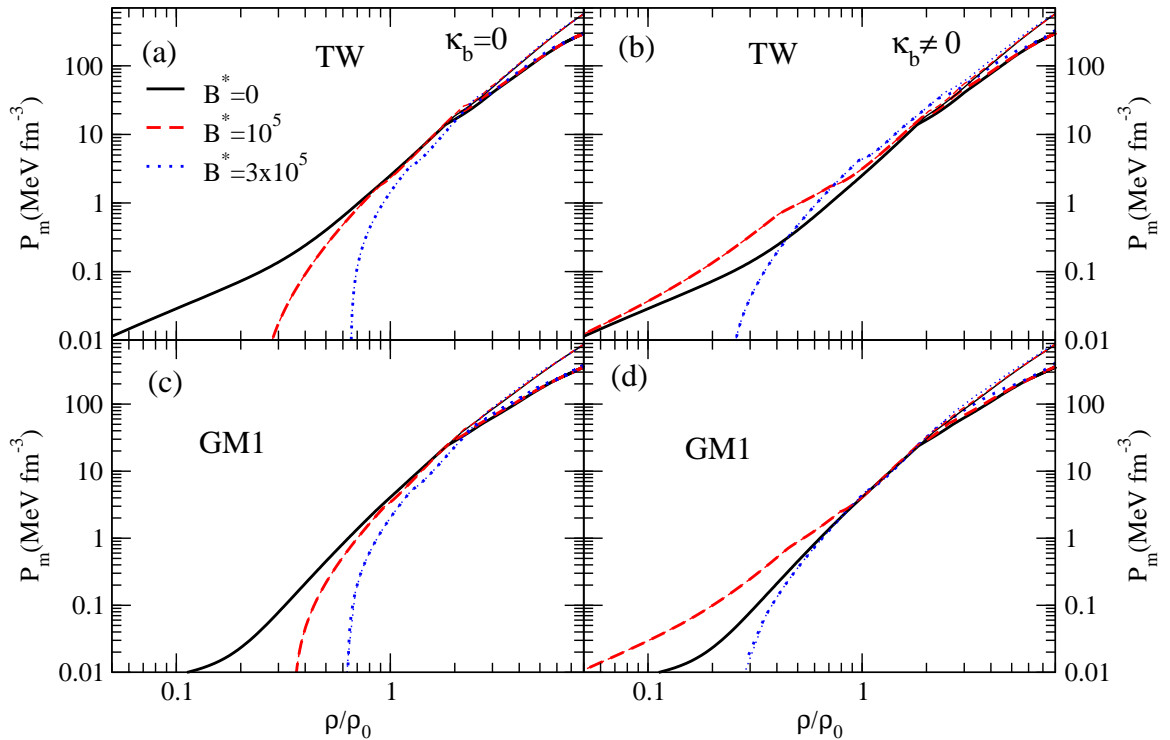


FIG. 1: EOS obtained with TW and GM1 models for neutrino free matter, and for several values of the magnetic field without (a) and (c) and with (b) and (d) AMM. Thick lines correspond to $x_\sigma = 0.6$ and thin lines to $x_\sigma = 0.8$. The kink in each EOS represents the onset of hyperons.

In Fig. 4 we show, for several values of magnetic field without including the AMM, for GM1 and TW models and for the two values of the hyperon-meson coupling constants, the strangeness fraction defined as

$$\tau_s^{HP} = \frac{\sum_b |q_s^b| \rho_b}{3\rho},$$

where q_s^b is the strange charge of baryon b , and is listed in Table I. The strangeness onset occurs around $2\rho_0$ and it has almost reached 0.275 (0.24) for GM1 and 0.23 (0.18) for TW, neutrino-free matter and $x_\sigma = 0.6$ ($x_\sigma = 0.8$). For $B = 0$ and for the neutrino-free matter, increasing the hyperon-meson couplings decreases the strangeness contents, and this suppression of strangeness is stronger in TW than GM1. However, if the neutrino trapping is imposed the strangeness fraction is smaller and a stronger reduction occurs for GM1 and for $x_\sigma = 0.8$.

For neutrino-free matter, the magnetic field reduces the strangeness fractions below a critical density that can be quite high, $6\rho_0$ or larger for the fields shown. This effect starts to be detected already for $B^* = 10^5$, which represents the threshold for the magnetic field effects to become significant, independently of the EOS [21]. However, the magnetic field enhances the strangeness fraction of neutrino-trapped matter. If the AMM are included the strangeness fraction behaves in the same way.

In Figs. 5, 6, 7, and 8, we present the particle fractions $Y_i = \rho_i^v/\rho$ as function of the baryon density ρ/ρ_0 for several values of the magnetic fields, obtained with TW model using two values of the hyperon-meson coupling constants $x_\sigma = 0.6, 0.8$ given in [35]. Figs. 5 and 7 are for neutrino-free matter and Figs. 6 and 8 for neutrino-trapped matter. For GM1 we get similar results.

First, we study the results obtained with the hyperon-meson coupling constant equal to $x_\sigma = 0.6$. For $B = 0$ neutrino free matter, shown in Fig. 5 (a), the proton fraction rises quickly with increasing density and reaches ~ 0.1 around $2\rho_0$ before the appearance of hyperons. Σ^- is the first hyperon to appear. In Fig. 5 (b) and (d), we show the results for $B^* = 10^5$ and $B^* = 3 \times 10^5$. At low densities, the fraction of nucleons and leptons are significantly affected by the magnetic field. The Landau quantization increases the proton abundance, and, therefore, the electron

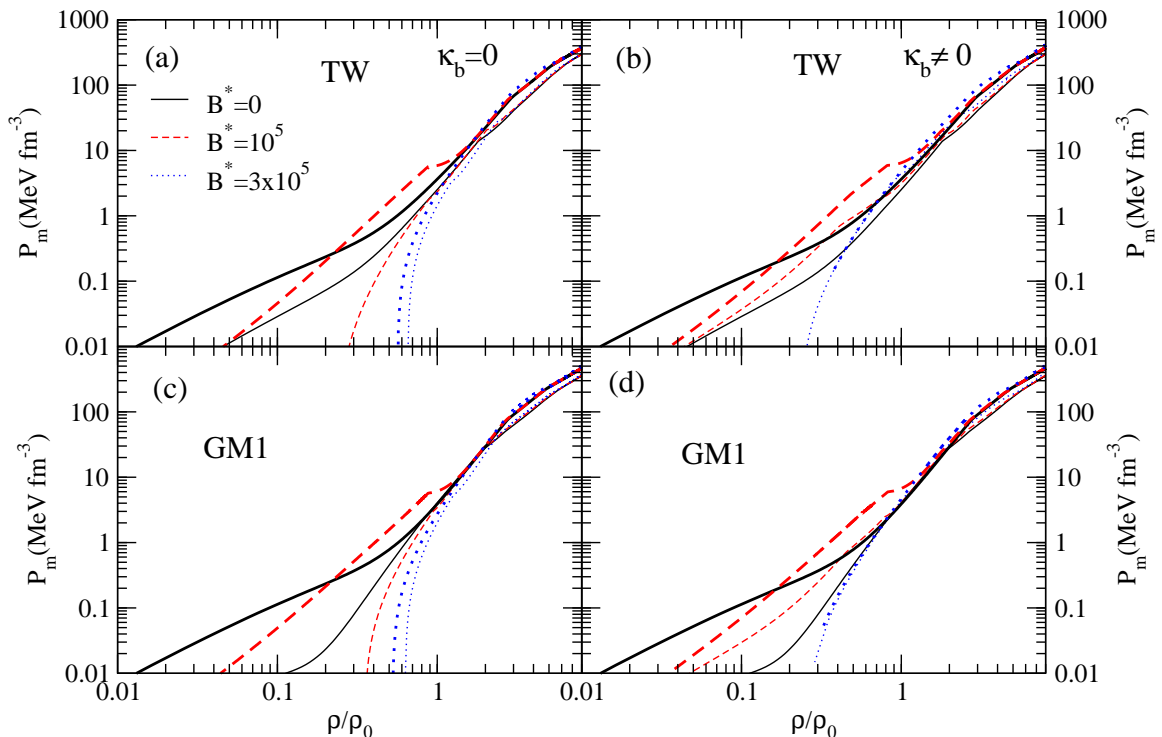


FIG. 2: EOS for TW and GM1 models and for $x_\sigma = 0.6$, without (a) and (c) and with (b) and (d) AMM. Thick lines for neutrino-trapped matter and thin lines for neutrino-free matter.

abundance due to the charge neutrality. In Fig. 9 we show for TW with $x_\sigma = 0.6$ the neutron, proton, electron and neutrino chemical potentials as a function of density for different values of the magnetic field. It is seen that the proton and neutron chemical potentials decrease with the increase of B . This is also the general tendency of leptons except for the larger densities. In the absence of AMM the reduction of the neutron chemical potential with an increase of the magnetic field is due to a reduction of the isospin asymmetry. The AMM will further reduce the neutron chemical potential. Landau quantization is the main explanation for a reduction of the proton chemical potential. As a consequence the threshold for the appearance of hyperons like Σ^- and Λ will occur at larger densities [21]. However, at densities above $\sim 5\rho_0$ the threshold densities for Σ^0 , Σ^+ , Ξ^- occur at smaller densities probably due to the smaller effective masses of these hyperons at large densities with strong magnetic fields. The inclusion of AMM, Fig. 5 (c) and (e), produces an even larger hyperon suppression at the lower densities.

TABLE III: The threshold density of hyperons in fm^{-3} when AMM is not included. for several values of magnetic field, for both GM1 and TW models and for neutrinos free and neutrino-trapped matter. We also identify, between brackets, the hyperon that appears at smaller densities.

B^*	Models	$x_\sigma = 0.6$		$x_\sigma = 0.8$	
		$Y_{Le} = 0$	$Y_{Le} = 0.4$	$Y_{Le} = 0$	$Y_{Le} = 0.4$
0	TW	0.275 (Σ^-)	0.441 (Λ)	0.301 (Σ^-)	0.514 (Λ)
	GM1	0.280 (Σ^-)	0.419 (Λ)	0.327 (Σ^-)	0.501 (Λ)
10^5	TW	0.311 (Σ^-)	0.438 (Λ)	0.338 (Σ^-)	0.516 (Λ , Σ^-)
	GM1	0.301 (Σ^-)	0.418 (Λ)	0.340 (Σ^-)	0.503 (Λ)
3×10^5	TW	0.358 (Σ^-)	0.445 (Σ^-)	0.385 (Σ^-)	0.506 (Λ , Σ^-)
	GM1	0.373 (Σ^-)	0.427 (Λ , Σ^-)	0.433 (Σ^-)	0.496 (Λ)

We consider now matter with trapped neutrinos. For $B = 0$, Fig. 6 (a), the proton and electron fractions are ~ 0.3 from low densities until the appearance of hyperons at $\sim 3\rho_0$ and, therefore, the neutrino fraction is ~ 0.1

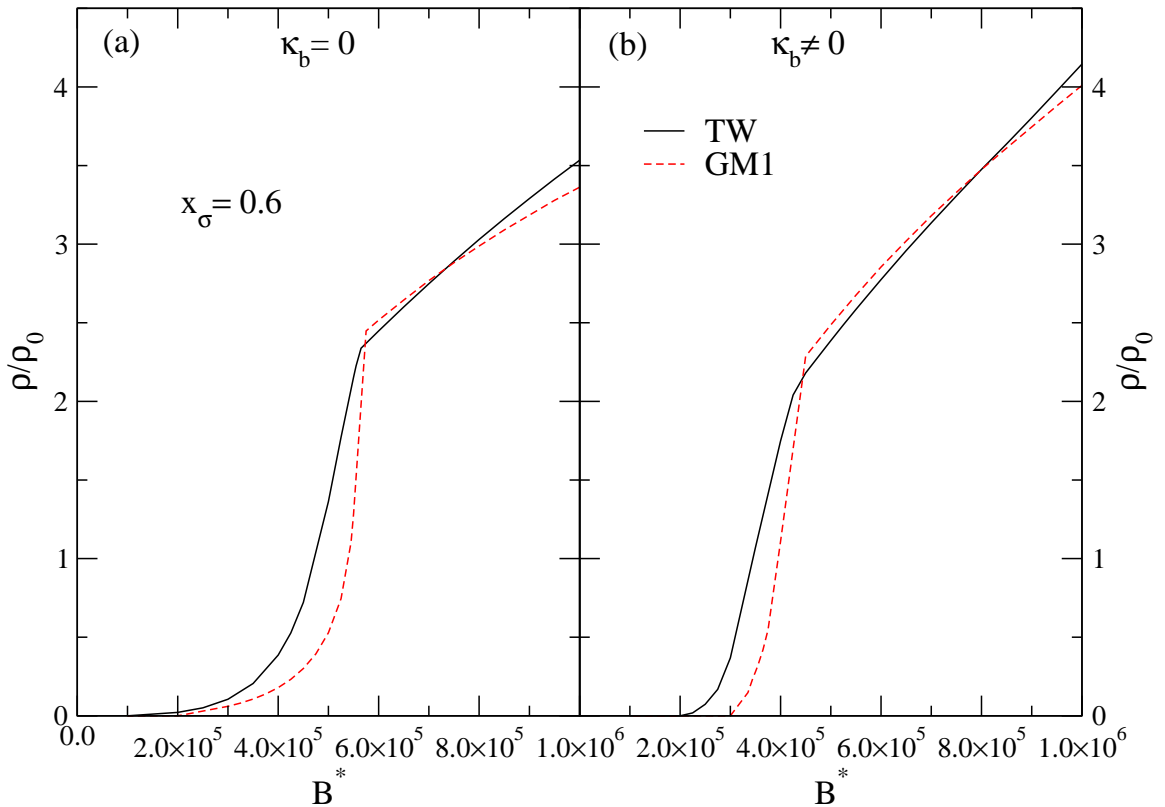


FIG. 3: Baryon density for which $\mu_{\nu_e} = 0$ versus B^* obtained for TW and GM1 models, with/without AMM and for $x_\sigma = 0.6$. Below this density it is not possible to impose $Y_{Le} = 0.4$.

TABLE IV: The threshold density of hyperons in fm^{-3} when AMM is included. for several values of magnetic field, for both GM1 and TW models and for neutrino free and neutrino-trapped matter. We identify, between brackets, the hyperon that appears at smaller densities.

B^*	Models	$x_\sigma = 0.6$		$x_\sigma = 0.8$	
		$Y_{Le} = 0$	$Y_{Le} = 0.4$	$Y_{Le} = 0$	$Y_{Le} = 0.4$
0	TW	0.275 (Σ^-)	0.441 (Λ)	0.301 (Σ^-)	0.514 (Λ)
	GM1	0.280 (Σ^-)	0.419 (Λ)	0.328 (Σ^-)	0.501 (Λ)
10^5	TW	0.291 (Σ^-)	0.433 (Λ)	0.315 (Σ^-)	0.500 (Λ)
	GM1	0.287 (Σ^-)	0.409 (Λ, Σ^-)	0.325 (Σ^-)	0.488 (Λ)
3×10^5	TW	0.344 (Σ^-)	0.389 (Σ^-)	0.373 (Σ^-)	0.457 (Σ^-)
	GM1	0.359 (Σ^-)	0.375 (Σ^-)	0.415 (Σ^-)	0.468 (Σ^-)

since we are imposing $Y_L = 0.4$. Λ is the first hyperon to appear for $B=0$. For $B^* = 10^5$ (see Fig. 6 (b)), the proton fraction is larger (~ 0.4) at the smaller densities, decreases to 0.3 for $\rho \sim \rho_0$ and stays approximately constant until the appearance of hyperons at $\sim 3\rho_0$. The neutrino fraction rises quickly with increasing density and reaches ~ 0.1 around ρ_0 and keeps, roughly, this value for larger densities. Λ is still the first hyperon to appear in this case. However, for $B^* = 3 \times 10^5$ (see Fig. 6 (d)), the proton fraction decreases slightly starting at ~ 0.4 at lower densities until the appearance of hyperons at $\sim 3\rho_0$. Σ^- is the first hyperon to appear almost at the same density as Λ . The neutrino fraction is almost zero at subsaturation densities, and rises, quickly, with increasing density, to ~ 0.2 around $6\rho_0$. The net effect of magnetic field is a neutrino suppression due to the larger proton and therefore electron fractions and to move the threshold density of the negatively charged baryons (*e.g.* Σ^-) to larger densities and the positively charged baryons to lower densities. This is due to a decrease (increase) of the chemical potentials of

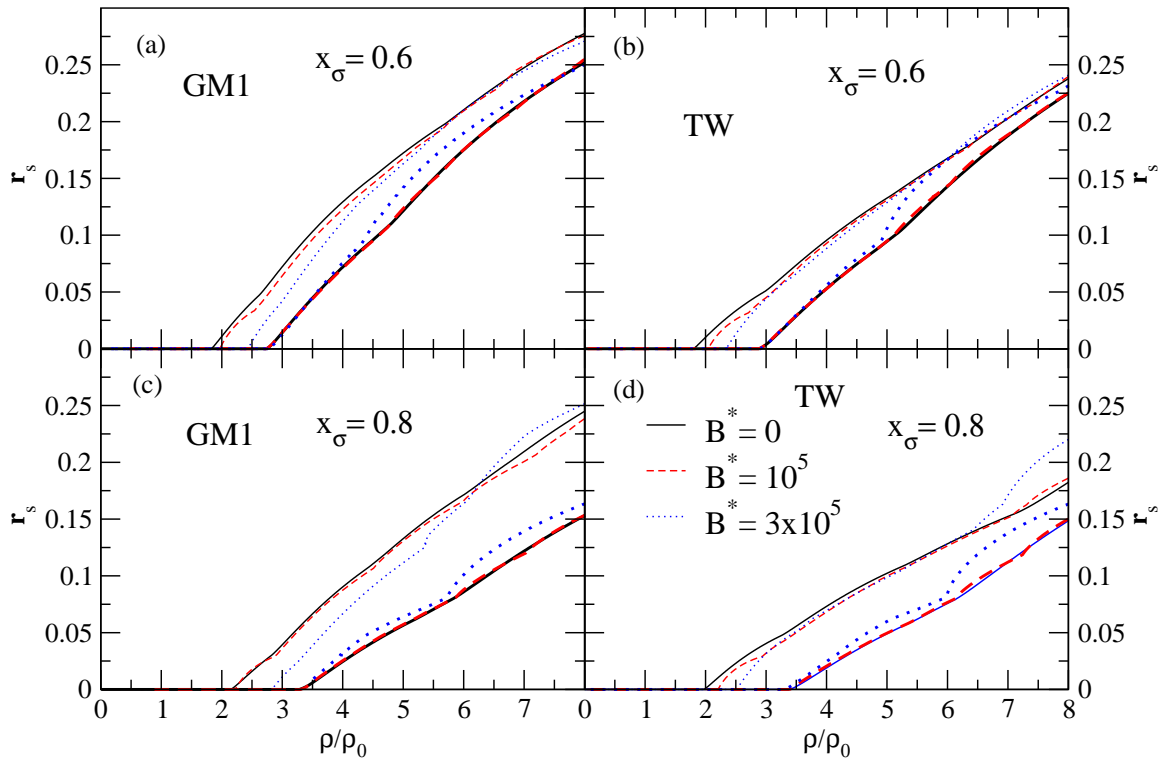


FIG. 4: Strangeness fraction as a function of the baryonic density, for several values of B , without AMM, and for GM1 and TW models. (a) and (b) for $x_\sigma = 0.6$ and (c) and (d) for $x_\sigma = 0.8$. Thick lines correspond to matter with trapped neutrinos and thin lines to neutrino-free matter.

negatively charged baryons (positively charged baryons) when the neutrino chemical potential is taken into account. In particular the onset of the Ξ^- occurs for densities larger than $8\rho_0$. The neutral baryons are not affected by the presence of neutrinos. In the presence of a strong magnetic field the overall effect of the neutrinos is smaller than for $B=0$.

For $x_\sigma = 0.8$, we obtain similar results and the main differences are: at high densities the onset of Ξ^- occurs at $\rho < 8\rho_0$, the onset of the Σ^- and Λ occurs at larger densities and hyperon fractions are smaller.

The effect of the magnetic field on the onset of hyperons, in both cases for neutrino free and neutrino trapped matter, is clearly shown in Tables III and IV, where we give the threshold density of the first hyperon, for TW and GM1 models and for $x_\sigma = 0.6$, and 0.8, without including the AMM (Table III) and including the AMM in (Table IV). The main conclusions for neutrino-free matter are: a) the hyperon onset occurs with the appearance of the Σ^- meson, both with and without AMM; b) the onset density generally increases with the increase of the magnetic field but for GM1 it may decrease for $B^* = 10^5$; c) the inclusion of AMM reduces the onset density of hyperons; d) the hyperon onset occurs at larger densities for $x_\sigma = 0.8$. For neutrino-trapped matter we conclude that: a) the onset density of hyperons is generally smaller when the magnetic field magnitude increases; b) for small fields, Λ is the first hyperon to appear but for large fields it is either Σ^- or Σ^- and Λ together.

In order to better understand the effect of the magnetic field on the neutrino trapping, we show in Fig. 10 the fraction of neutrinos for several values of magnetic field. For $B = 0$, the neutrino fraction decreases at low densities and starts to increase after the onset of hyperons because with the hyperon onset the electron fraction gets smaller. For $B^* = 5 \times 10^4$ and $B^* = 10^5$, the neutrino fraction is affected by the Landau quantization of electrons, and oscillates around the $B = 0$ results, when AMM are not included. At low densities the main effect of magnetic field is the suppression of neutrinos. For $B^* > 10^5$, the neutrino fraction is lowered at low densities and enhanced at higher densities. However, when the AMM are included, the abundance of neutrinos is only slightly reduced for $B^* = 5 \times 10^4$ and $B^* = 10^5$, while for $B^* > 10^5$ the neutrino suppression is strong, *e. g.* for $B^* = 3 \times 10^5$ there are no neutrinos at a density below the saturation density. We conclude, therefore, that the abundance of neutrinos in the presence of

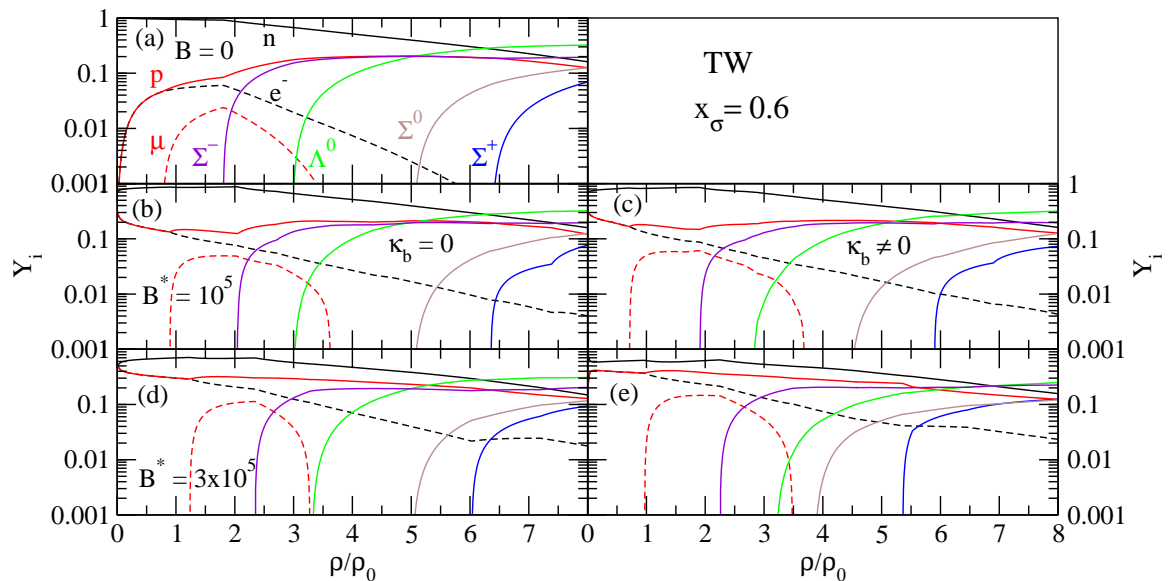


FIG. 5: Baryon fraction versus baryon density obtained with TW model for $x_\sigma = 0.6$ and neutrino-free matter.

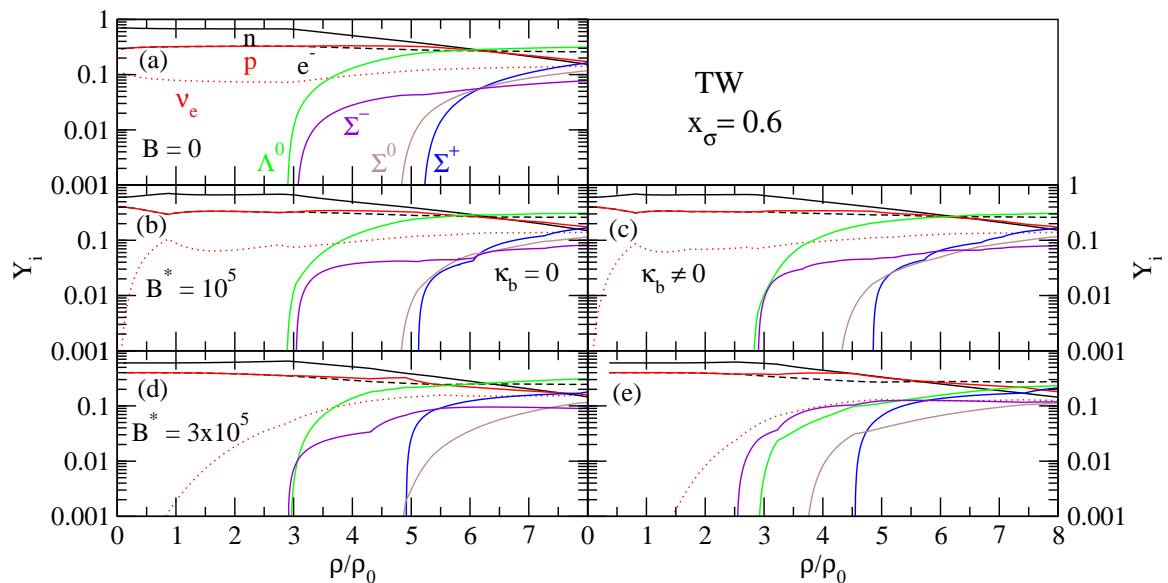


FIG. 6: Baryon fraction versus baryon density obtained with TW model for $x_\sigma = 0.6$, and neutrino-trapped matter.

strong magnetic fields has a strong suppression at low densities.

In order to study the effect of the magnetic field on the properties of the stars described by the EOS discussed above with neutrino trapping, we must consider a density dependent magnetic field, which is not larger than 10^{15}G at the surface. We will do this in the next section.

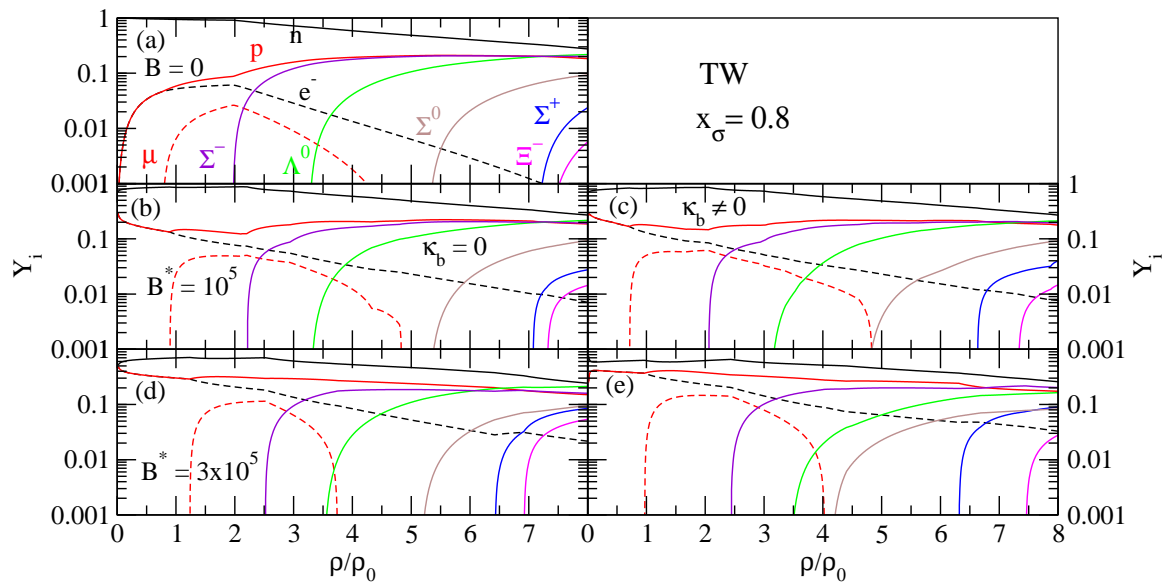


FIG. 7: Baryon fraction versus baryon density obtained with TW model, for $x_\sigma = 0.8$ and neutrino-free matter.

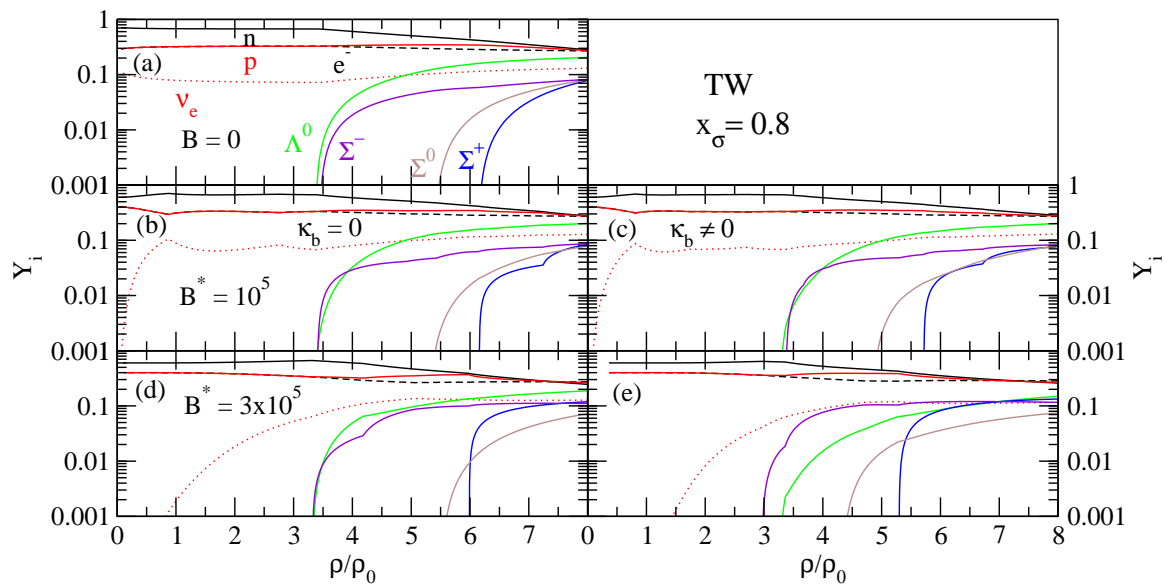


FIG. 8: Baryon fraction versus baryon density obtained with TW model, for $x_\sigma = 0.8$ and neutrino-trapped matter.

B. Baryon density-dependent magnetic field

Since, to date, there is no information available on the interior magnetic field of the star, we will assume that the magnetic field is baryon density-dependent as suggested by Ref. [41]. The variation of the magnetic field B with the

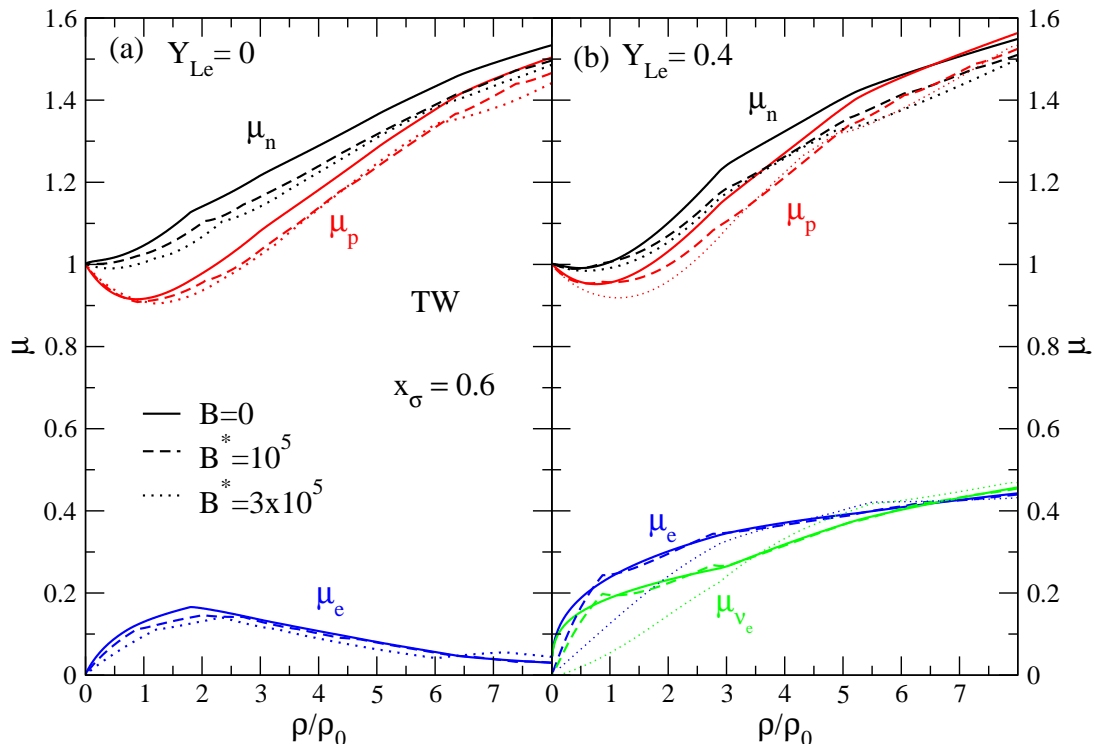


FIG. 9: Chemical potentials versus baryon density obtained with TW model, for several values of magnetic field, without AMM, and for $x_\sigma = 0.6$ and for (a) neutrino-free matter; (b) neutrino-trapped matter.

baryon density ρ from the center to the surface of a star is parametrized [30, 41, 42] by the following form

$$B\left(\frac{\rho}{\rho_0}\right) = B^{\text{surf}} + B_0 \left[1 - \exp\left\{-\beta\left(\frac{\rho}{\rho_0}\right)^\gamma\right\}\right], \quad (22)$$

where ρ_0 is the saturation density, B^{surf} is the magnetic field at the surface taken equal to 10^{15} G, in accordance with the values inferred from observations and B_0 represents the magnetic field at large densities. The parameters β and γ may be chosen in such way that the field decreases fast or slowly with the density from the center to the surface. In this work, we will use one set of value ($\beta = 0.05$ and $\gamma = 2$) allowing a slowly varying field. The magnetic field will be given in units of the critical field $B_e^c = 4.414 \times 10^{13}$ G for the electron, so that $B_0 = B_0^* B_e^c$. We further take B_0 as a free parameter to check the effect of different fields. A detailed discussion about the variation of the magnetic field with the baryon density may be found in Ref. [30].

In this section, we will only present the results for the density-dependent relativistic model TW and we will take for the hyperon-meson coupling constants $x_\sigma = 0.6$. Furthermore, in all the figures, we will only show the results obtained without including the baryonic AMM, because for the intensity of the magnetic fields considered, its contribution to the EOS is negligible. The effect of the AMM is non negligible for $B^* > 10^5$ [43], and is larger for the smaller densities, but according to [21] these values will never be reached inside the star.

In Fig. 11, we show the total pressure P , see Eq. (21), as a function of the baryon density for the magnetic field strengths $B^* = 0, 10^5$, and 3×10^5 . The results with neutrino-trapped and neutrino-free matter are plotted with thick and thin lines, respectively. The EOS with neutrino trapping is stiffer than the neutrino free EOS, both with and without magnetic field. In Fig. 11(a), we only show the results without the AMM because for the fields considered almost no effect is introduced by the AMM. In Fig. 11(b) we show the difference between the EOS with and without AMM for neutrino free matter (thin line) and matter with trapped neutrinos (thick line). The differences are of the order of $20 \text{ MeV}/\text{fm}^3$ for a density $8\rho_0$. However, according to [21] the magnetic field inside a stable star cannot be larger than $1\text{-}3 \times 10^{18}$ G and therefore, for $B_0^* = 3 \times 10^5$ the central density will not go beyond $\rho \sim 3\rho_0$, as seen from

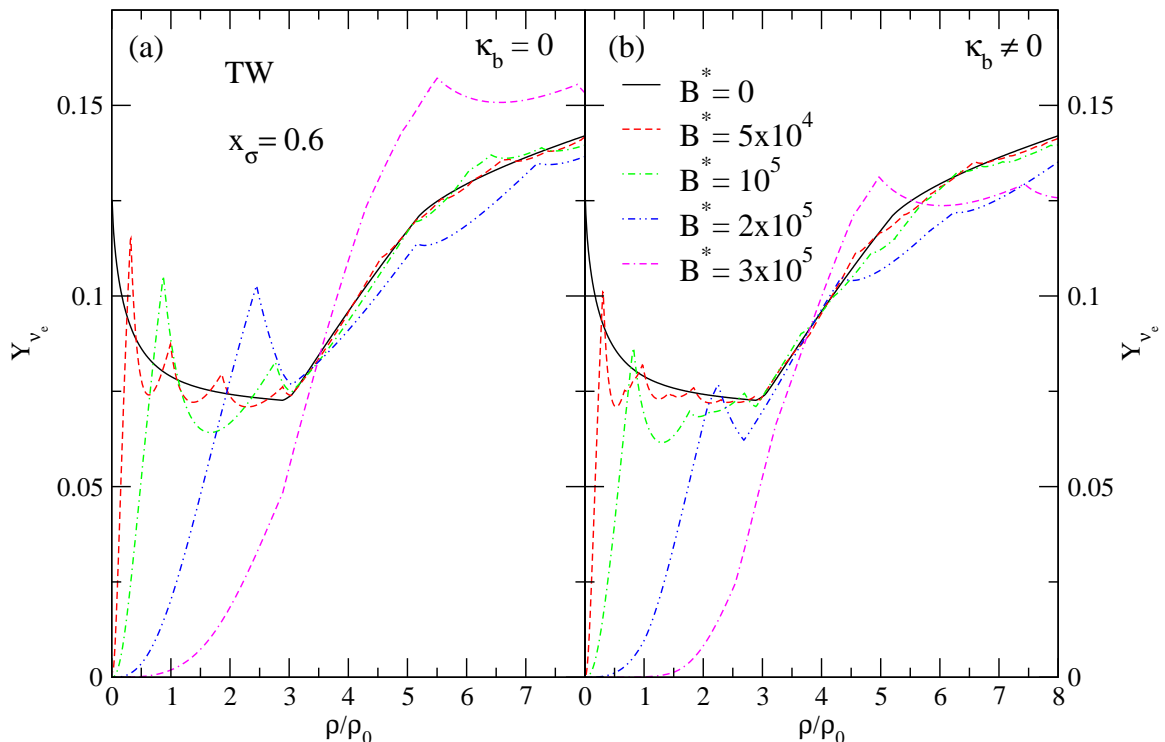


FIG. 10: Neutrino fraction versus baryon density obtained with TW model, for several values of the magnetic field without/with including AMM and for $x_\sigma = 0.6$.

Fig. 11(c) where we have plotted the density dependent magnetic field according to the parametrization given in (22). The differences introduced by AMM for $\rho \sim 3\rho_0$ are smaller than 1%.

We have also studied the baryonic and leptonic composition of the stars. In Fig. 12 we plot the lepton and the baryon fractions for neutrino free matter (left column) and for neutrino trapped matter (right column) for TW model. We show the particle fractions for the smallest and the largest magnetic fields considered in the present work. The shaded regions in the figures represent the densities of the star for the maximum magnetic fields in stable star configurations obtained in [21] ($B \sim 1 - 3 \times 10^{18}$ G) if it lies within the range of densities shown. We conclude that the main effect of magnetic fields with the intensity considered is the appearance at high densities of a larger leptonic fraction. Due to the contribution of the magnetic field to the total energy-momentum tensor, the contribution of matter becomes smaller when the magnetic field increases and, therefore, the fraction of strangeness in the star is strongly reduced because the larger contributions of hyperons for the star would come from the larger densities which are not reached in the presence of a strong magnetic field.

IV. CONCLUSIONS AND OUTLOOKS

In the present work we have studied the effect of a strong magnetic field on the EOS and the star properties when neutrinos are trapped in the star. We have used two different relativistic mean-field models, one with constant coupling parameters, GM1, and the other with density dependent coupling parameters, TW. We have also considered two sets of hyperon-coupling parameters. The main conclusions of the work do not depend either on the model or on the strength of the hyperon-couplings.

The phase of trapped neutrinos in the life of a proto-neutron star occurs while the stellar matter is still warm [20, 40], and, therefore, a finite temperature calculation should have been done. However, we do not expect that temperature will change the main conclusions of the present work. In fact, in several works [20, 44, 45] it has been shown that the star properties such as mass and radius do not depend much on temperature.

We have shown that a strong magnetic field suppresses the presence of neutrinos at low densities. It was also shown that although strangeness is suppressed by the presence of neutrinos, if the star has a strong magnetic field this suppression is smaller. The magnetic field affects in a different way the charged and neutral baryons and it may affect the density order at which they appear. For neutrino free matter, Σ^- is the first hyperon to appear at the smallest densities. However, for neutrino trapped matter, Λ is the first hyperon to appear except for the largest field considered when we may have Σ^- or Σ^- and Λ .

We have studied some properties of stars with trapped neutrinos and strong magnetic fields. We have considered a density dependent magnetic field with the magnitude 10^{15} G at the surface, and determined the EOS of the star and the particle fractions as a function of the density. One of the main consequences of the presence of the magnetic field is the reduction of the strangeness fraction in the star. A similar conclusion with respect to other exotic components such as a quark core [30], or kaon condensation [23] had already been pointed out. As a consequence the magnetic field reduces the possibility of formation of a black-hole after the outflow of neutrinos, since it is the onset of exotic matter in neutrino free matter that may induce a black-hole formation if the EOS becomes too soft.

Acknowledgments

We would like to thank João da Providência for many helpful and elucidating discussions. This work was partially supported by FEDER and Projects PTDC/FP/64707/2006 and CERN/FP/83505/2008, and by COMPSTAR, an ESF Research Networking Programme.

-
- [1] B. Paczyński, *Acta Astron.* 42, 145 (1992).
 - [2] R. C. Duncan and C. Thompson, *Astrophys. J.* 392, L9 (1992); C. Thompson and R. C. Duncan, *MNRAS* 275, 255 (1995).
 - [3] V. V. Usov, *Nature* 357, 472 (1992).
 - [4] A. K. Harding and D. Lai, *Rep. Prog. Phys.* 69, 2631 (2006)
 - [5] SGR/APX online Catalogue, <http://www.physics.mcgill.ca/~pulsar/magnetar/main.html>
 - [6] C. Kouveliotou, S. Dieter, T. Strohmayer, J. van Paradijs, G.J. Fishman, C.A. Meegan, K. Hurley, *Nature* 393, 235 (1998).
 - [7] N. K. Glendenning, *Compact Stars*, Springer-Verlag, New-York, 2000.
 - [8] R. Knorren, M. Prakash, and P. J. Ellis, *Phys. Rev. C* 52, 3470 (1995)
 - [9] J. Schaffner and I. N. Mishustin, *Phys. Rev. C* 53, 1416 (1996); Jurgen Schaffner-Bielich and Avraham Gal, *Phys. Rev. C* 62, 034311 (2000)
 - [10] M. Baldo, G. F. Burgio, and H.-J. Schulze, *Phys. Rev. C* 58, 3688B (1998); *Phys. Rev. C* 61, 055801 (2000).
 - [11] I. Vidaña, A. Polls, A. Ramos, M. Hjorth-Jensen, and V. G. Stoks, *Phys. Rev. C* 61, 025802 (2000); I. Vidaña, A. Polls, A. Ramos, L. Engvik, and M. Hjorth-Jensen, *Phys. Rev. C* 62, 035801 (2000).
 - [12] Y. Yamamoto, S. Nishizaki, and T. Takatsuka, *Nucl. Phys. A* 691, 432c (2001); Shigeru Nishizaki, Yasuo Yamamoto and Tatsuyuki Takatsuka, *Prog. Theor. Phys.* 105, 607 (2001); *ibid*, *Prog. Theor. Phys.* 108, 703 (2002).
 - [13] F. Hofmann, C. M. Keil, and H. Lenske, *Phys. Rev. C* 64, 034314 (2001)
 - [14] N. K. Glendenning, *Phys. Rev. C* 64, 025801 (2001).
 - [15] H. Shen, *Phys. Rev. C* 65, 035802 (2002).
 - [16] H. Shen and Z. L. Zhang, *Chin. Phys. Lett.* 20, 650 (2003).
 - [17] S. Pal, M. Hanauske, I. Zakout, H. Stöcker, and W. Greiner, *Phys. Rev. C* 60, 015802 (1999).
 - [18] P. K. Panda, D. P. Menezes, and C. Providência, *Phys. Rev. C* 69, 025207 (2004).
 - [19] H. Heiselberg and M. Hjorth-Jensen, *Phys. Rep.* 328, 237 (2000).
 - [20] M. Prakash, I. Bombaci, M. Prakash, P. J. Ellis, J. M. Lattimer, and R. Knorren, *Phys. Rep.* 280, 1 (1997).
 - [21] A. Broderick, M. Prakash and J. M. Lattimer, *Phys. Lett. B* 531, 167-174 (2002).
 - [22] S. L. Shapiro and S. A. Teukolsky, *Black holes, white dwarfs and neutron stars*, Wiley-interscience New York, 1983.
 - [23] P. Yue, H. Shen, *Phys. Rev. C* 77, 045804 (2008)
 - [24] P. Yue, F. Yang, and H. Shen, *Phys. Rev. C* 79, 025803 (2009).
 - [25] Debora P. Menezes and C. Providência, *Phys. Rev. C* 69, 045801 (2004).
 - [26] A. Li, G. F. Burgio, U. Lombardo, W. Zuo W, *Phys. Rev C*, 74, 055801 (2006); Sarmistha Banik and Debades Bandyopadhyay, *Phys. Rev. C* 63, 035802 (2001); I. Vidaña, I Bombaci, and I Parenti, *J. Phys. G: Nucl. Part. Phys.* 31, S1165 (2005).
 - [27] D. Bandyopadhyay, S. Pal, and S. Chakrabarty, *J. Phys. G: Nucl. Part. Phys.* 24, 1647 (1998); S. Pal, D. Bandyopadhyay, and S. Chakrabarty, *J. Phys. G: Nucl. Part. Phys.* 25, L117 (1999).
 - [28] D. P. Menezes, M. Benghi Pinto, S. S. Avancini, A. Pérez Martínez, and C. Providência, *Phys. Rev. C* 79, 035807 (2009).
 - [29] A. Rabhi, C Providência, and J. da Providência, *J. Phys. G: Nucl. Part. Phys.* 35,125201 (2008).
 - [30] A. Rabhi, H. Pais, P. K. Panda, and C Providência, *J. Phys. G: Nucl. Part. Phys.* 36,115204 (2009).
 - [31] C. Fuchs, H. Lenske and H. Wolter, *Phys. Rev. C* 52, (1995) 3043.

- [32] S. Typel and H. H. Wolter, Nucl. Phys. **A656**, 331 (1999).
- [33] F.X. Wei, G.J. Mao, C.M.Ko,L.S. Kisslinger, H. Stoecker and W. Greiner, J. Phys. G: Nucl. Part. Phys. 32, 47 (2006).
- [34] F. de Jong and H. Lenske, Phys. Rev. C 57, 3099 (1998).
- [35] N. K. Glendenning and S. A. Moszkowski, Phys. Rev. Lett. 67, 2414 (1991).
- [36] J. Schaffner-Bielich and A. Gal, Phys. Rev. C 62 (2000) 034311.
- [37] J. Schaffner-Bielich, Phys. Rev. Lett. 89 (2002) 171101-1.
- [38] E. Friedman, A. Gal, Phys. Rep. 452 (2007) 89.
- [39] M. Chiapparini, M. E. Bracco, A. Delfino, M. Malheiro, D. P. Menezes, C. Providência, Nucl. Phys. A 826, 178 (2009).
- [40] A. Burrows and J.M. Lattimer, Astrophys. J. 307, 178 (1986).
- [41] D. Bandyopadhyay, S. Chakrabarty, and S. Pal, Phys. Rev. Lett. 79. 2176 (1997).
- [42] G.-J. Mao, A. Iwamoto and Z.-X. Li, Chin. J. Astron. Astrophys. Vol.3, No 4, 359-374 (2003).
- [43] A. Broderick, M. Prakash and J. M. Lattimer, Astrophys. J. 537, 351 (2000).
- [44] D. P. Menezes and C. Providência, Phys. Rev. C 68, 035804 (2003).
- [45] Debora P. Menezes and C. Providência, Phys. Rev. C 70, 058801 (2004).

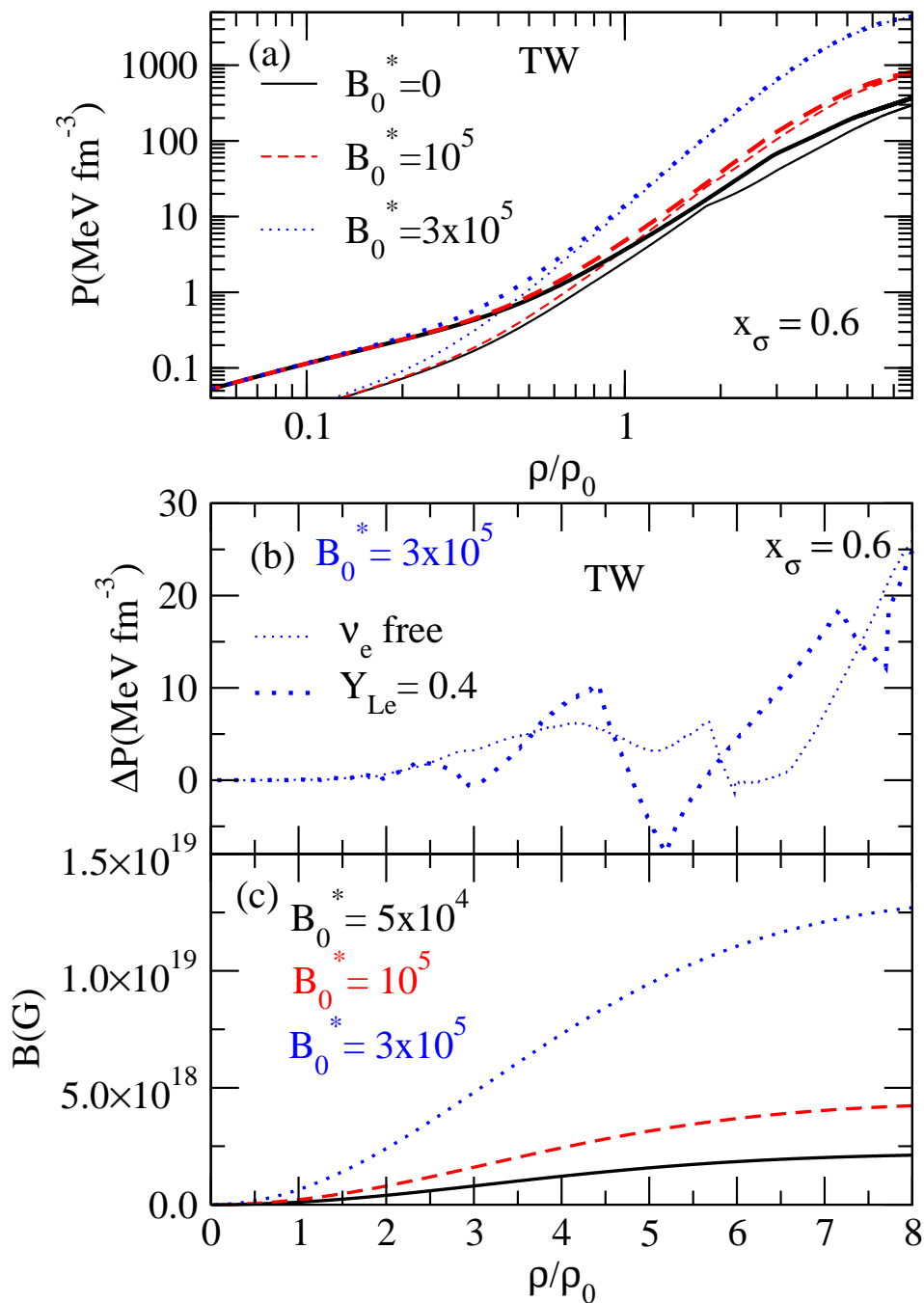


FIG. 11: EOS for stellar matter for TW model without/with neutrino trapping, for $x_\sigma = 0.6$, using a slowly varying parametrization of B (a) for several values of magnetic field and without AMM; (b) for $B_0^* = 3 \times 10^5$ the difference between the EOS including AMM and the EOS without AMM. Thin lines correspond to neutrino-free matter and thick lines to neutrino-trapped matter. In (c) we plot the intensity of the magnetic field versus density for $B_0^* = 5 \times 10^4$ (2.20×10^{18} G), $B_0^* = 10^5$ (4.41×10^{18} G), and $B_0^* = 3 \times 10^5$ (1.32×10^{19} G).

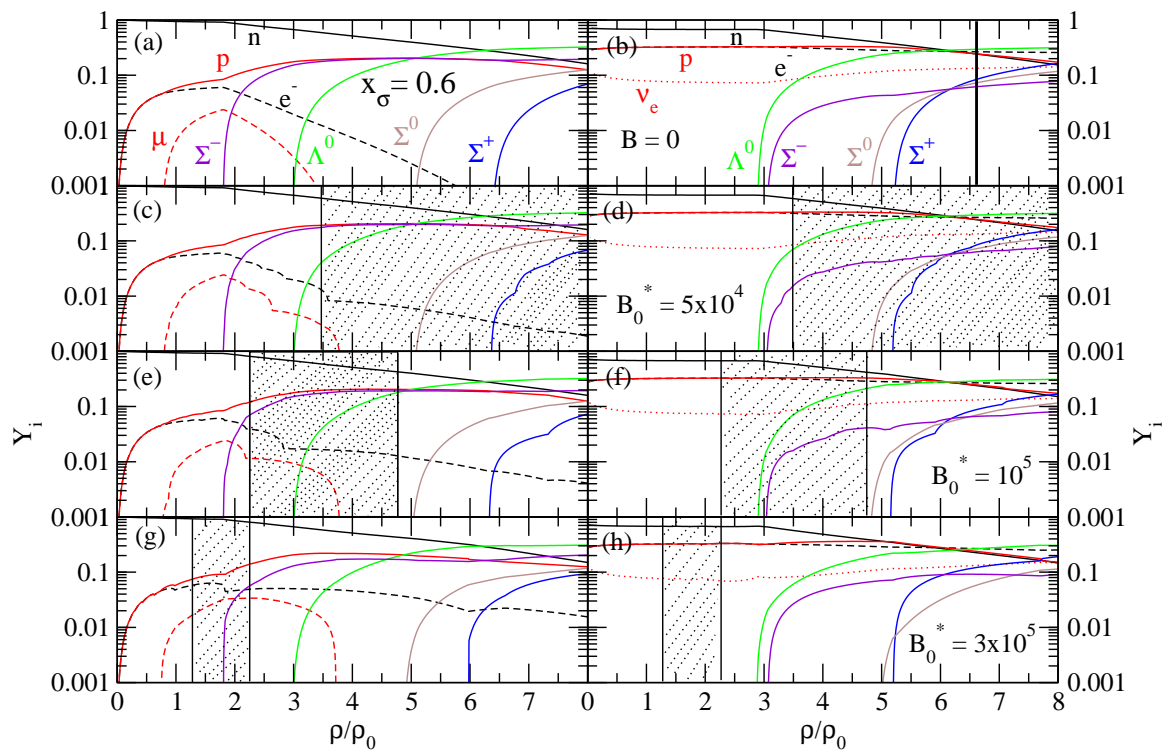


FIG. 12: Baryon fraction versus density obtained with TW model with/without neutrino trapping, for several values of the magnetic field, using a slowly varying parametrization of B , and without AMM. Figures (a), (c), (e), and (g) are for neutrino free and (b), (d), (f), and (h) for neutrinos trapped. In figures (c), (d), (e), (f), (g), and (h), shaded regions correspond to the baryon densities for which the magnetic field is between $1-3 \times 10^{18}$ G.